

Optical Critical Dimension Measurement and Illumination Analysis Using the Through-focus Focus Metric

Ravikiran Attota[#], Richard M. Silver, Michael R. Bishop^{*}, and Ronald G. Dixon

Precision Engineering Division, National Institute of Standards and Technology, Gaithersburg, MD 20899

^{}International SEMATECH, Austin, TX 78741*

ABSTRACT

In this paper we present a unique method of evaluating the angular illumination homogeneity in an optical microscope using the through-focus focus metric. A plot of the sum of the mean square slope throughout an optical image as the target moves through the focus is defined as the through-focus focus metric. Using optical simulations we show that the angular illumination inhomogeneity causes the through-focus focus metric value to proportionately increase at specific focus positions. Based on this observation, we present an experimental method to measure angular illumination homogeneity by evaluating the through-focus focus metric values on a grid across the field of view. Using the same through-focus focus metric, we present a detailed study to measure critical dimensions with nanometer sensitivity with the aid of simulations.

Keywords: Optical Critical Dimension (OCD) Metrology, Through-focus focus metric, Angular Optical illumination, Köhler factor

1. INTRODUCTION

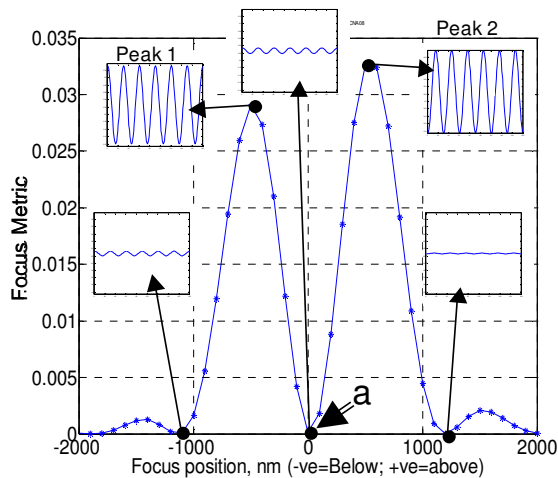


Figure 1. A typical simulated TFFM profile for line array exhibiting proximity effects. Insets are intensity profiles at the indicated focus positions. The optical image has high contrast at peaks 1 and 2, while it has very low contrast at point “a” as shown by an arrow. Parameters for simulation: Line width=140 nm; Line height=200 nm; Pitch=600 nm; Illumination NA =0.4; NA=0.8; Wavelength=546 nm. Si lines on Si substrate. Zero position represents top of the substrate.

The focus metric, as defined here, is the sum of the mean square slope throughout an optical image. A plot of the focus metric as the target moves through the focus is called through-focus focus metric (TFFM). The TFFM profile typically has a single peak when imaging a single line. The image at the peak focus metric value is usually considered to be the best focused image. However, the TFFM of a line grating, that experiences interference of the scattered field, exhibits multiple TFFM peaks as shown in Fig. 1. Previous observations of this interference phenomenon on silicon line gratings were presented in Ref. (1) using optical simulations. The shape of the TFFM profile depends on several factors (2,3). It depends on the target parameters such as critical dimension (CD), line height, pitch, sidewall angle and its optical properties. It also depends on microscope settings such as the illumination numerical aperture, the collection numerical aperture, the illumination wavelength, the optical aberrations and the quality/homogeneity of illumination.

Application of the TFFM profile for CD analysis and experimental results showing nanometer sensitivity of the method were presented in Refs. (1,2,4). A recent independent investigation by Ku et. al. (5) has produced similar results. In the present paper we present a detailed study of the TFFM method not only for nanometer CD sensitivity, but also for CD measurement.

The dependence on theoretical simulations to enhance experimental optical CD measurement accuracy has continually increased as CDs have decreased. To have accurate simulations the optical instrument needs to be characterized as accurately as possible to determine the appropriate input parameters for the simulation. Often, imperfect illumination is the dominant factor in optical CD/overlay measurement errors. In addition to uniform spatial illumination intensity, angular illumination symmetry is necessary to obtain a symmetric experimental intensity profile in order to compare it with the simulation, where symmetric angular illumination is assumed.

We have also applied TFFM profile analysis to evaluate the illumination at the sample. This approach enables the determination of the angular intensity distribution. The result can be used to either correct the experimental illumination in the optical tool or to identify the location in the field of view where the best illumination symmetry is present for subsequent optical measurements (6). Additionally, the measured angular distribution of the illumination can be used as input for the simulations. This approach is expected to improve the agreement between the experiments and the simulations resulting in more accurate optical CD and overlay measurements.

2. ILLUMINATION ANALYSIS

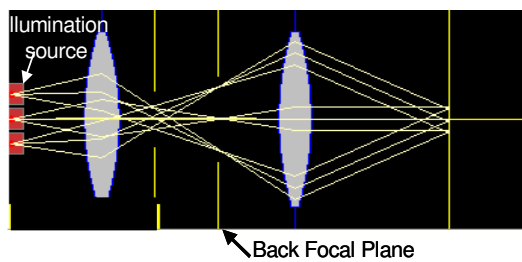


Figure 2. A simplified schematic of a Köhler illumination. Each point on the back focal plane produces an illumination plane wave at a specific angle

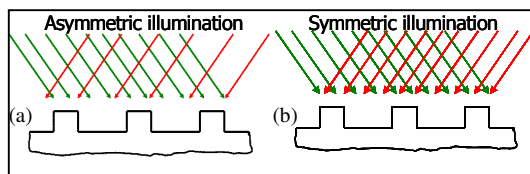


Figure 3. (a) Asymmetric and (b) Symmetric angular illumination schemes.

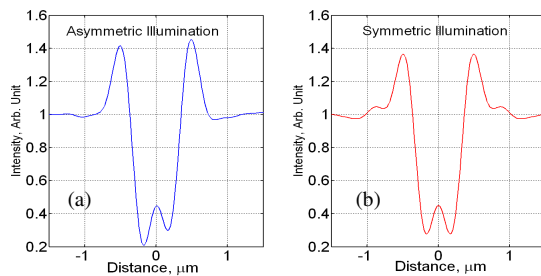


Figure 4. Simulated intensity profiles of an isolated line for symmetric and asymmetric illuminations. Line width=200 nm; Line height=200 nm; Illumination NA=0.4; collection NA=0.8, Wavelength=546 nm; Si line on Si substrate.

Proper illumination is essential in virtually all optical metrology applications. Köhler illumination is one common approach to obtaining accurate illumination. A simplified schematic of a Köhler illumination is shown in Fig. 2. Each point on the back focal plane produces an illumination plane wave at a specific angle. Historically, obtaining uniform spatial illumination intensity across the field of view by employing a Köhler illumination scheme was considered sufficient. However, for the three-dimensional objects encountered in several semiconductor industry applications, obtaining Köhler illumination with homogenous spatial intensity is necessary, but not sufficient. It is also necessary to achieve angular illumination homogeneity. Figure 3 shows two illumination schemes. Both of the illumination schemes have uniform spatial illumination intensity across the field of view. However, the illumination scheme in Fig. 3(a) has asymmetric angular illumination, while the illumination scheme in Fig. 3(b) has symmetric illumination. In a recent comprehensive analysis of Köhler illumination, asymmetry in the angular illumination has been defined as Köhler factor 2 (KF2).

For a detailed analysis of Köhler illumination errors and the associated Köhler factors refer to (7).

The effects of asymmetric illumination on the resulting optical images (intensity profiles) were studied using optical simulations. A rigorous coupled wave-guide analysis* model (8) was used for this purpose. The intensity profile of an isolated line was simulated for both symmetric and the asymmetric illumination cases. The symmetric illumination produces a symmetric intensity profile as shown in Fig. 4(a), while the asymmetric illumination produces an asymmetric intensity profile as shown in Fig. 4(b). As can be expected, asymmetric illumination results in inaccurate measurement results. Therefore, it is critical to obtain symmetric angular illumination for accurate optical CD and overlay measurements. In fact it is fundamental to reducing tool-induced-shift.

*Usage of this model does not imply endorsement of NIST

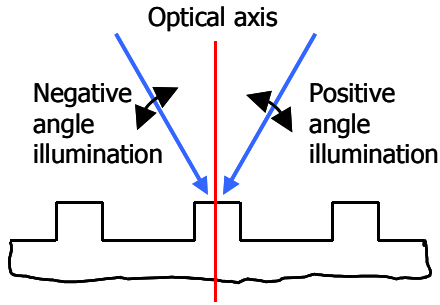


Figure 5. Division of illumination for the analysis.

2.1 Angular Illumination Symmetry Evaluation Using the Through-focus Focus Metric. In the Köhler illumination configuration shown in Fig. 2 the target is illuminated by plane waves from all of the angles that lie within the angles allowed by the illumination NA. For angular illumination symmetry analysis, the Köhler illumination in the optical microscope is divided as shown in Fig. 5. All the angles of illumination to the left of the optical axis are bundled into negative angles of illumination and all the angles of illumination to the right of the optical axis are bundled into positive angles of illumination. The total illumination is the sum of all of the negative and the positive angles of illumination.

Using an incoherent source in the Köhler illumination scheme, each individual plane wave produces an image. The final image is the incoherent sum of all the images formed by all the individual illuminating plane waves. Based on the separation of angles shown in Fig. 5, it is therefore implicit that the final image is formed by the incoherent sum of the images formed by all negative and all positive angles of illumination.

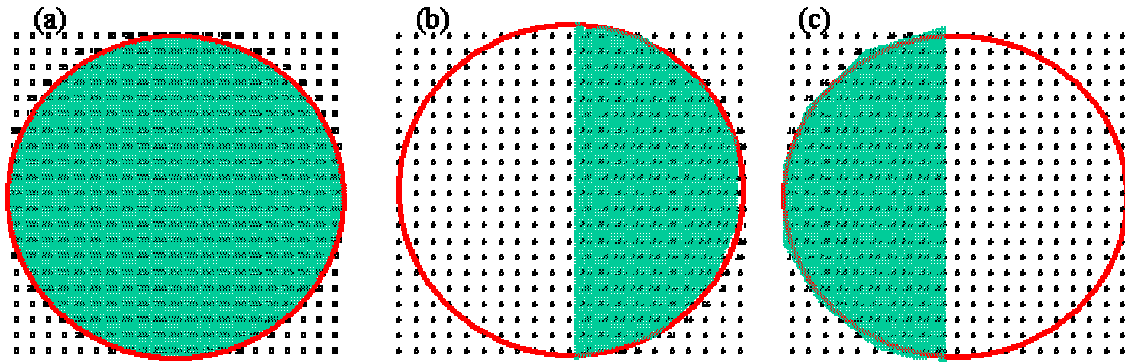


Figure 6. Back focal plane intensity is represented by matrices in the simulations. Simulations were made using (a) complete circular, (b) right semicircular and (c) left semicircular illuminations at the back focal plane.

2.2 Simulations. Using the division of incident illumination shown in Fig. 5, further optical simulations were carried out. In the RCWA model used for the simulations presented here, a matrix of numbers as shown in Fig. 6 represents the back focal plane illumination. Each number in the matrix produces an illumination plane wave at a particular angle. The magnitude of the number determines the intensity of the illuminating plane wave. In the simulation, the final image is obtained by the incoherent sum of all the images formed by each plane wave.

Through-focus simulations of a line grating were made using three types of back focal plane fill factors. In the first illumination set up, a circular back focal plane was illuminated with uniform intensity (Fig. 6(a)). This results in all angles of equal intensity illumination. In the second type of fill factor (Fig. 6(b)), only the right half of the back focal plane was uniformly illuminated, resulting in only the negative angles of illumination. In the third type (Fig. 6(c)), only the left half of the back focal plane was uniformly illuminated resulting in the positive angles of illumination. The through-focus image intensity profiles for the three types of illuminations are shown in Fig. 7. Each window shows image intensities for a single through-focus focus position. The profile at the top of each window is the result of illumination from all angles (first type). The two overlapping profiles at the bottom of each window are individually formed by the negative angles (second type) or the positive angles (third type) of illumination.

The following observations can be made from the through-focus images shown in Fig. 7. Intensity profiles from only the negative or only the positive angles of illumination appear different. Their shape changes with focus position. The

final image formed by all incident angles is the incoherent sum of the images formed by only the negative and only the positive incident angles of illumination. The sum of the slope contained in an intensity profile is a measure of the image contrast. When the maximum or the minimum intensities in the images formed by only the negative and only the positive angles of illumination overlap, the resultant final image has the highest contrast as shown in window 11 in Fig. 7. Window 16 shows the instance where there is minimum overlap in the peak values which results in the lowest contrast final image. Images formed by only the negative and only the positive angles of illumination by themselves do not produce low contrast images. However, when the intensities are added they can produce a low contrast final image. Window 16 image focus position corresponds to point 'a' in Fig. 1. By moving the sample focus position in small incremental steps, a certain point is reached about the point 'a' where the sum of the negative and the positive illumination images produce an almost constant intensity response. This situation results in an extremely low final image intensity contrast i.e. the intensity profile is nearly flat. The focus metric value (i.e. sum of the slopes) of this image is nearly zero. Further examination of the images at this focus position provides additional insight to the illumination analysis.

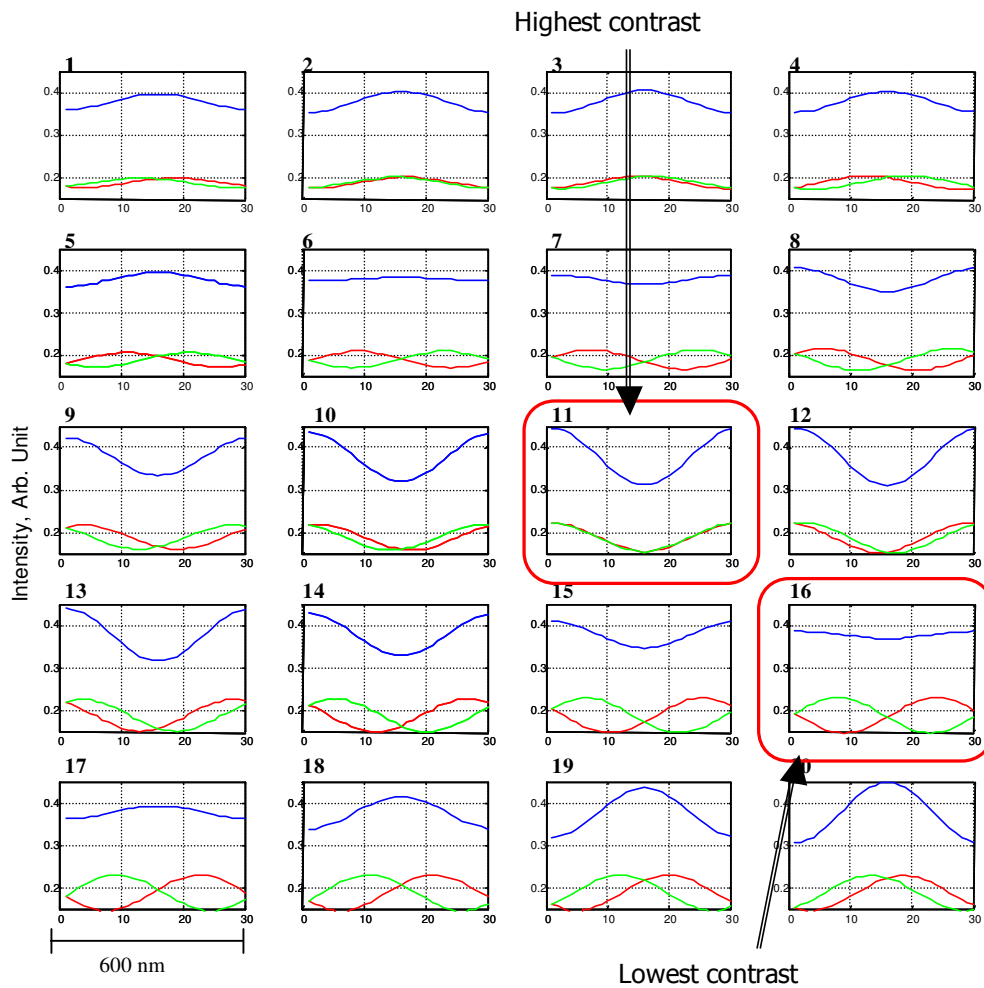


Figure. 7. Simulated through-focus image intensity profiles of a line grating. The lower overlapping curves in each window are the intensity profiles for only the negative angles and only the positive angles of illumination. The above curve is the intensity profile for all the angles of illumination. Each window is at different focus position. Y-axis is the intensity in arbitrary units, x-axis is the distance. Profile of only one pitch length is shown in the figure. Input parameters for the simulation: Line width = 200 nm, Line height = 200 nm, Pitch = 600 nm, Illumination NA = 0.4, Collection NA = 0.8, Illum. Wavelength = 546 nm, Si line on Si substrate.

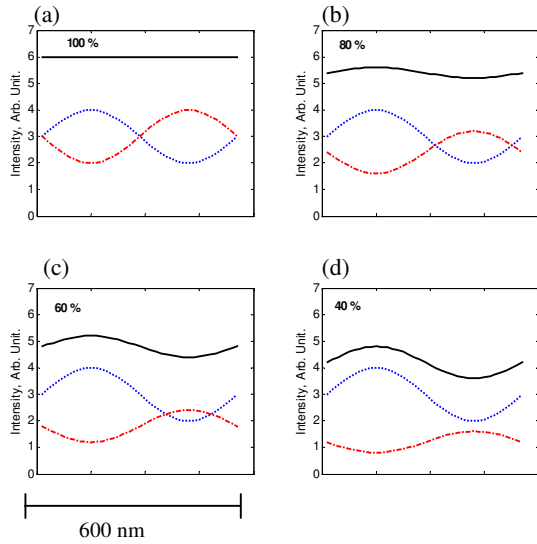


Figure. 8 Schematic intensity profiles for the negative angles (dotted), the positive angles (dot-dash), and all the angles (solid) of illumination at the focus position ‘a’ (Fig. 1). Percentage of the left half intensity compared to the right half is indicated in the figure. Length of the profile equals to one pitch.

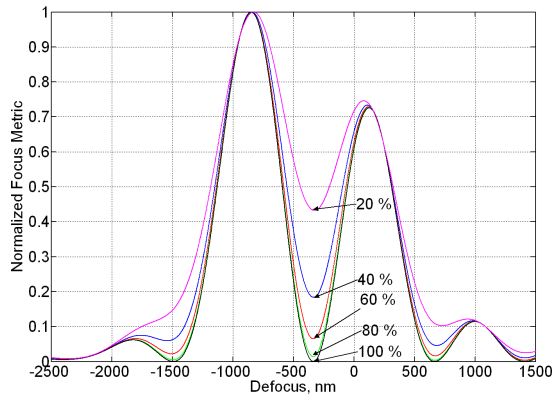


Figure. 9. TFFM profiles at reduced left half back focal plane intensity. Percentage of the left half intensity compared to the right half is indicated in the figure.

wavelength and at 50X objective magnification. Through focus images were acquired for two perpendicular target orientations. In the analysis, the entire field of view was divided into 50 rows and 50 columns. TFFM profiles were calculated for each of the 50 x 50 locations. The resulting normalized minimum focus metric values at point ‘a’ were obtained for each of the 50 x 50 locations for the two perpendicular orientations. A plot of the minimum focus metric values across the field of view indicates the asymmetry in the angular illumination.

The experimental results for the poorly aligned microscope are presented in Fig. 10. In the three-dimensional image on the left side, the x-y axes represent the field of view and the z-axis represents the magnitude of the focus metric at point ‘a’ (Fig.1). The results show that the poorly aligned microscope has large angular illumination asymmetry across the field of view. For this configuration of the microscope an arrow shows the location in the field of view with the lowest

Uniform illumination of the entire back focal plane produces the constant intensity profiles schematically shown in Fig. 8(a). The dotted line is the image intensity profile produced by only the negative incident angles, the dot-dash line is the image intensity produced by only the positive incident angles, and the solid line is the image intensity profile produced by all the incident angles of illumination. In this example both the negative and the positive incident angles are illuminated at 100 % intensity. As explained above, this results in an extremely low contrast final image. The focus metric has near zero value. However, when the intensity of all the positive incident angles is uniformly reduced to 80 % of the negative incident angles, the sum of the negative and the positive illumination profiles no longer produce a constant intensity profile as shown in Fig. 8(b). This results in a higher contrast final image. Further reduction of all the positive incident angles uniformly increases the contrast of the final image as shown in Figs. 8(b) to 8(d). Consequently, the focus metric value, which is a measure of the total slope content, increases with increasing contrast. This analysis of the simulation shows that increasing intensity differences between the negative and the positive incident angles of illumination increases the focus metric value at the point ‘a’ (Fig. 1). The simulated TFFM profiles using different levels of the negative and the positive incident angle intensity are shown in Fig. 9. As expected, the focus metric value at point ‘a’ increased with increasing intensity difference between the negative and the positive incident angles of illumination.

2.3 Experimental Verification. From the above discussion it was observed that the magnitude of the focus metric at point ‘a’ (Fig. 1) was an indication of the asymmetry in the angular illumination intensity. Based on this observation an experimental attempt was made to analyze the asymmetry in the angular illumination for a poorly aligned and a well-aligned Köhler illuminated microscope. The experimental details are as follows. A 100 μm x 100 μm scatterometry target with approximately 229 nm wide, 230 nm tall, 540 nm pitch array of lines was imaged through the focus at 100 nm increments using an optical microscope with 0.8 collection NA, 0.4 illumination NA, 546 nm illumination

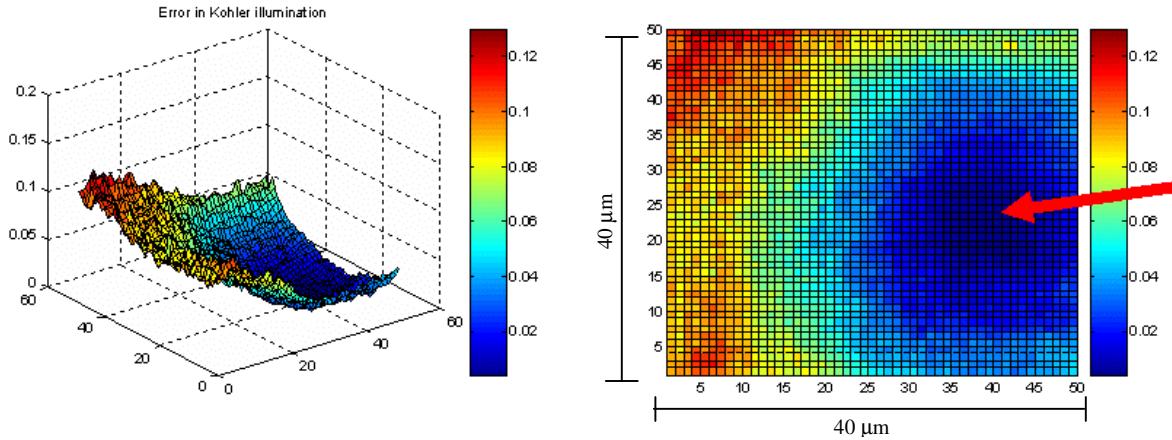


Figure 10. The experimental evaluation of the asymmetry in the angular illumination for the poorly aligned microscope. The X-Y axes represents a $40\ \mu\text{m} \times 40\ \mu\text{m}$ field of view and the Z-axis is the focus metric in the left side figure. The right side figure is a two dimensional projection of the left side three dimensional figure. The best symmetric illumination location in the field of view is shown by an arrow. A target with approximately $229\ \text{nm}$ wide, $230\ \text{nm}$ tall, $540\ \text{nm}$ pitch array of lines ($100\ \mu\text{m} \times 100\ \mu\text{m}$) was imaged using an optical microscope with 0.8 collection NA, 0.4 illumination NA and $546\ \text{nm}$ illumination wavelength at $50\times$ objective magnification.

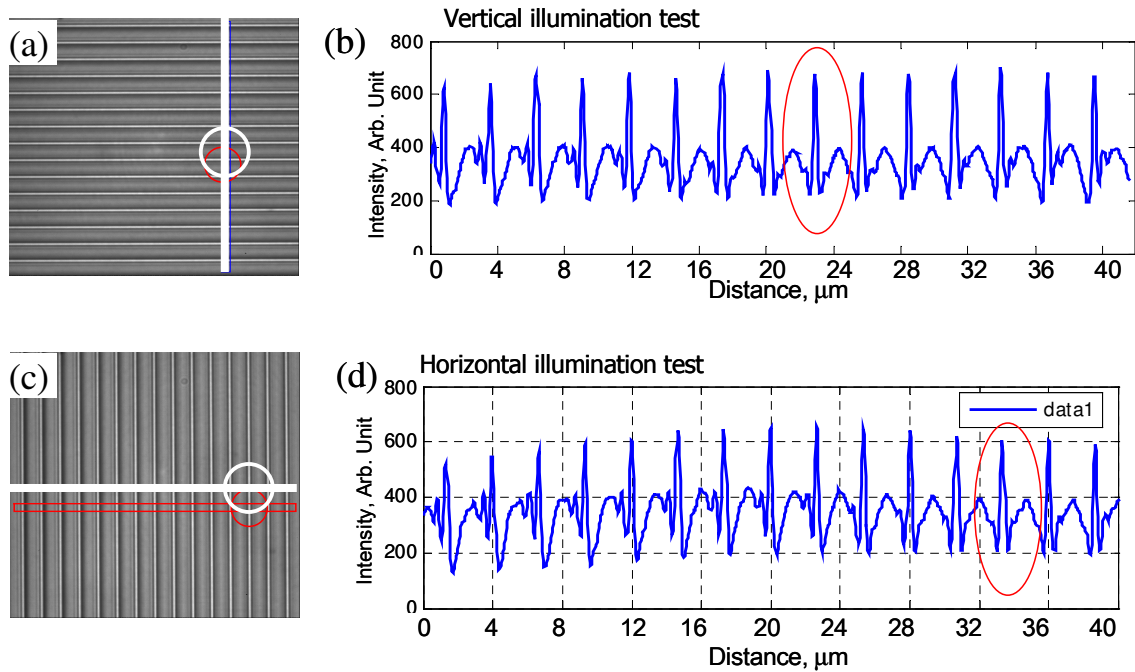


Figure 11. Experimental verification of asymmetry in the angular illumination for the poorly aligned microscope. (a) and (c) are the optical images of the horizontal and the vertical line gratings respectively. (b) and (d) are the intensity profiles at the locations shown by rectangles in (a) and (c).

value of the focus metric. Based on the discussion above, this location in the field of view for this microscope setup shows the best angular illumination symmetry, i.e. an image of a symmetric line at this location should produce the best symmetric profile (from the discussion used for Fig. 4). Other locations in the field of view, because of their asymmetric illumination will produce asymmetric image intensity profiles. The asymmetry in the illumination increases the further one moves from the location of best symmetry. It can also be observed that for this microscope setup the location for best angular symmetry does not coincide with the center of the field of view.

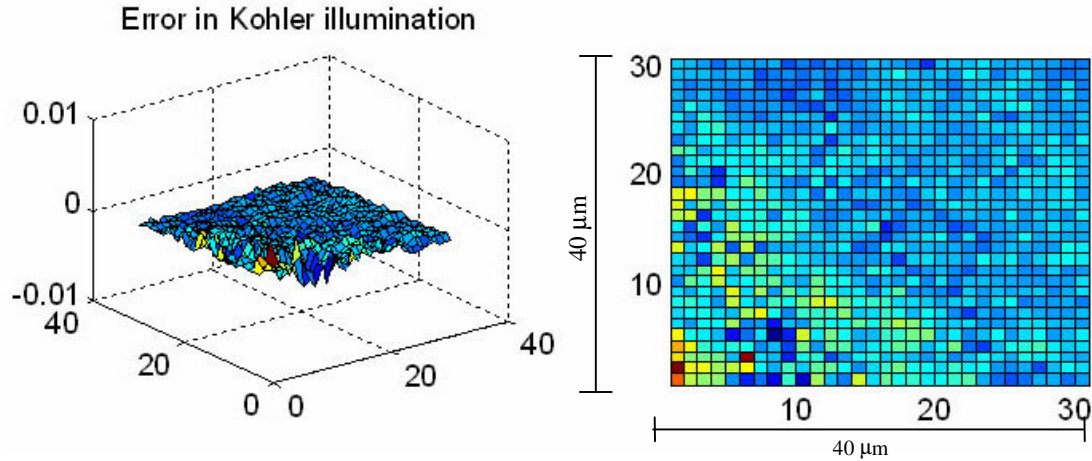


Figure 12. Experimental evaluation of asymmetry in the angular illumination for the well aligned microscope. X-Y axis represents 40 μm x 40 μm field of view and Z-axis is the focus metric in the left side figure. The right side figure is a two dimensional projection of the left side three dimensional figure. A target with approximately 155 nm wide, 230 nm tall with 600 nm pitch array of lines (100 μm x 100 μm) was imaged using an optical microscope with 0.8 collection NA, 0.38 illumination NA and 546 nm illumination wavelength at x50 objective magnification.

Experiments were conducted to evaluate the validity of the illumination analysis for the poorly aligned microscope. A line grating scatterometry target with approximately 229 nm wide, 230 nm tall, 2500 nm pitch array of lines was imaged in two perpendicular orientations at the best focus position using an optical microscope with 0.8 collection NA, 0.4 illumination NA, 546 nm illumination wavelength, and 50X objective magnification. The optical images and the corresponding intensity profiles at the locations shown in the optical images are shown in Fig. 11. Two important observations can be made from this experimental result. Although this microscope setup has good uniform spatial intensity as can be observed by the reasonably flat intensity profile, it has extremely poor angular illumination symmetry. All of the lines except for one show asymmetrical intensity profiles for both the horizontal and the vertical lines. From the above discussion this indicates angular illumination asymmetry at all the locations except where the symmetric intensity profiles are present. The locations of the most symmetric intensity profiles are highlighted using ellipses for both the horizontal (Fig. 11(b)) and the vertical (Fig. 11(d)) lines. Circles show the corresponding locations in the optical images (Figs. 11(a) and (c)). Comparison of Fig.10 and Fig. 11 shows that the locations of the circles in the field of view (Fig. 11) match the best angular illumination symmetry location analysis shown in Fig. 10, confirming this angular illumination analysis.

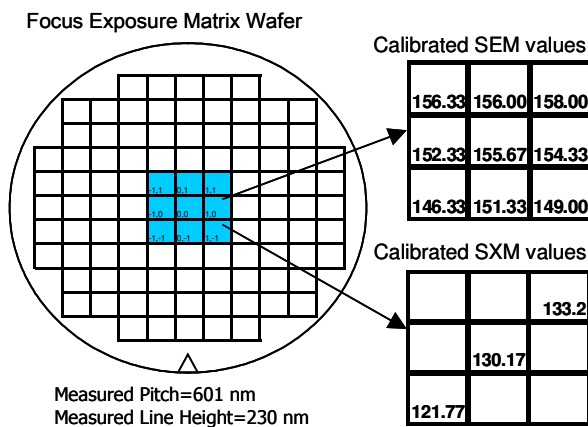


Figure 13. Measured bottom CD values in nm, using CDSEM and CDAFM (SXM).

The well-aligned microscope has much better angular illumination symmetry as shown in Fig. 12. However, even this microscope setup has some angular asymmetry at the lower left corner in the field of view. Here the entire field of view was divided into 30 rows by 30 columns for the analysis.

3. EVALUATION OF THE CRITICAL DIMENSION USING THE THROUGH-FOCUS FOCUS METRIC

3.1 The TFFM Experiments. Experimental evaluation of critical dimensions using the optical TFFM is presented in this section. An etched Si, focus exposure matrix wafer was used for this study. A 100 μm X 100 μm scatterometry target with a nominal CD of 100 nm and a pitch of 600 nm was selected for the CD analysis. The CDs and pitches of the targets in several dies were measured using a calibrated

critical dimension-scanning electron microscopy (CDSEM) . From these results, a selection of dies with small variation in the bottom CD were identified for further analysis. The line height and the sidewall shape was obtained using a calibrated atomic force microscopy (CDAFM). These values are presented in Fig. 13.

The selected targets were imaged through the focus in 100 nm size increments using an optical microscope with 0.8 collection NA, 0.39 illumination NA, 546 nm illumination wavelength, and 50X objective magnification. Each experiment was repeated at least three times. The mean, normalized TFFM experimental profiles are presented in Fig. 14 along with the measured CDSEM values and their standard deviations. This shows good experimental sensitivity to nanometer changes in CD using the TFFM method.

3.1 The TFFM Experiments and the Simulations Comparison. A critical element of the experiment to simulation comparisons is accurate knowledge of the experimental conditions so as to perform simulations with the correct input parameters. The needed input parameters for the simulations can be divided into two broad categories: 1) target related parameters and 2) microscope related parameters. The required target related input parameters are CD (starting point values), height, pitch, sidewall shape and optical properties. Except for CD, all of the input parameters can be reasonably well characterized using the appropriate instrumentation. The microscope related input parameters needed are illumination NA, collection NA, illumination wavelength, and illumination homogeneity. The microscope used in the work presented in this section had reasonably good illumination homogeneity (Fig. 12). The other measured microscope parameters are presented above. However, the illumination NA needs some further explanation.

An alternative method to infer the illumination NA by comparing the simulated and the experimental TFFM profiles was presented in a previous publication (2). The TFFM curves have proven to be very sensitive to the illumination NA. Since the TFFM depends on the illumination NA, it can be evaluated experimentally provided all the other input parameters are well characterized and known. In Ref. (2), using a traditional geometrical method, where the largest angle of illumination is measured, the measured illumination NA was found to be nominally 0.5. However, the effective illumination NA measured by matching the experimental TFFM with the simulated TFFM was 0.42. Subsequent to the study presented here, a major cause of this effective lower illumination NA on the tool used in this work was identified as significant differences in the intensity transmission of the ‘s’ and ‘p’ polarized light at larger incident angles. For more information on this, refer to Silver et al. (9).

Based on the discussion in the preceding paragraph, it is likely that the effective illumination NA for the microscope used in the current study is less than the 0.39 value measured using the standard geometrical approach. However, the exact effective lower illumination NA is not known. As a result, two unknowns need to be evaluated: CD and illumination NA. However, approximate values for both the CD and the illumination NA are known. Based on these starting-point values, we can attempt to evaluate the CDs.

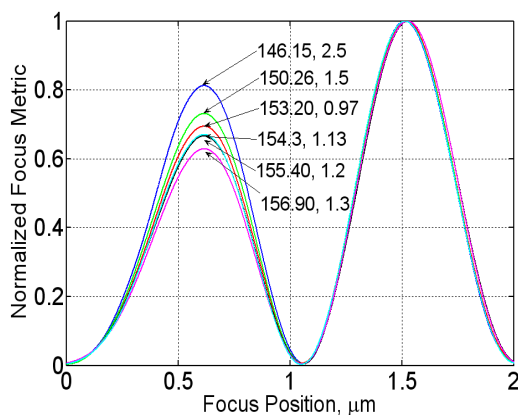


Figure 14. Mean experimental TFFM profiles for the 6 target locations selected normalized to the bigger focus metric peak. SEM measured CD values and their standard deviations are indicated in the figure in nanometer.

The measured CDSEM and SXM CD values have approximately 25 nm offset with respect to one another (Fig. 13). However, the die-to-die differences in the CD values are nearly the same for the two methods, indicating that both methods have good precision and sensitivity. However, there are uncertainties in the accuracy of the measurements.

Using the available input parameters, TFFM profiles were obtained by simulation for CDs varying from 125 nm to 175 nm and illumination NAs varying from 0.35 to 0.39. For the range of illumination NAs modeled, qualitative agreement between the simulated TFFM profiles for 125 nm and 135 nm CDs and the experimental TFFM profiles (see Figs. 14 and 15) is not achieved. However, qualitative agreement between the simulated TFFM profiles (see Fig. 15) and the experimental profiles is obtained for CDs in the range of 145 nm, 155 nm, 165 nm and 175 nm CDs. The match between the simulations and experimental results is optimized with a

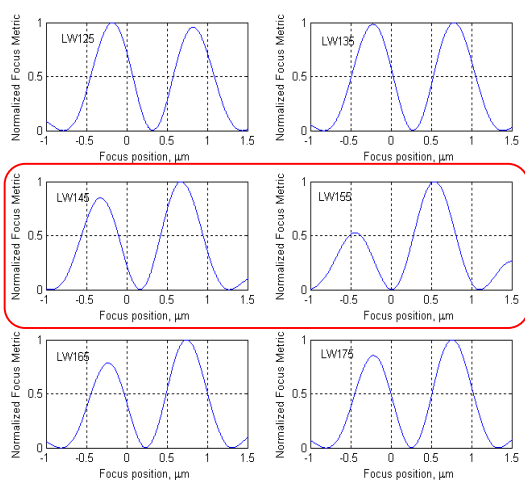


Figure 15. Simulated TFFM profiles for 125 nm, 135 nm, 145 nm, 155 nm, 165 nm and 175 nm bottom CDs at 0.37 illumination NA. Other input parameters are: Line height=230 nm, Pitch=601 nm, collection NA=0.8, Illum. Wavelength=546 nm, Si lines on Si substrate. Sidewall profile is shown in Fig. 13

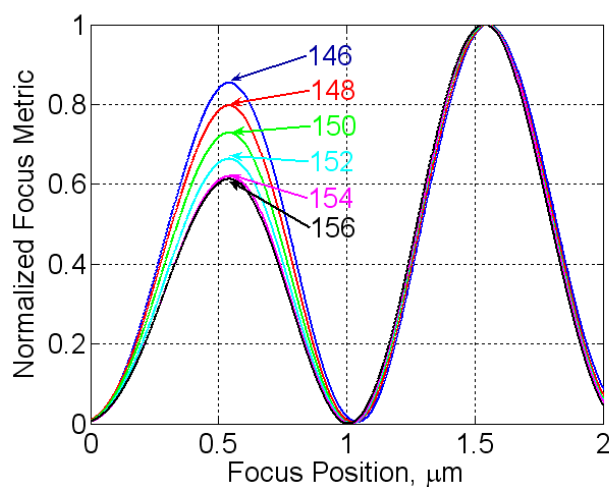


Figure 16. Simulated TFFM profiles for 146 nm to 156 nm bottom CDs at 0.36 illumination NA. Other input parameters are: Line height=230 nm, Pitch=601 nm, collection NA = 0.8, Illum. Wavelength=546 nm, Si lines on Si substrate.

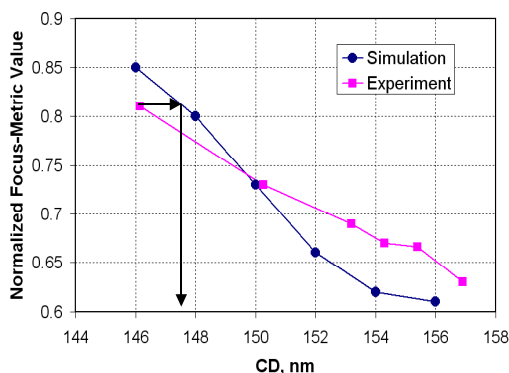


Figure 17. Plot of normalized left peak intensity vs. CD for the simulations and the experiments.

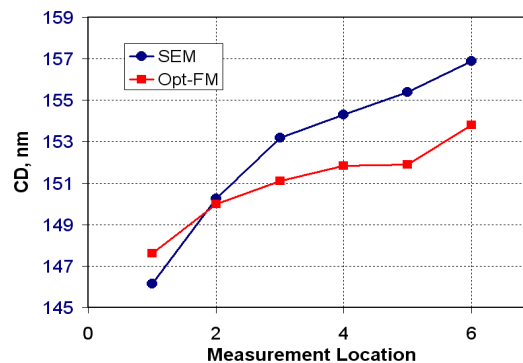


Figure 18. Measured CD values using SEM, and the through-focus focus metric method using the optical microscope.

choice of illumination NA of 0.37, which is a reasonable choice based on the effective NA discussion above. A closer look at the experimental TFFM curves shows that the left peak focus metric value decreases with increasing CD. A decreasing left peak focus metric value is only observed for the line width simulations between 135 nm and 155 nm CD. For the lines with CDs between 155 nm and 175 nm, the left peak focus metric value increases. Therefore, this analysis indicates that the experimental targets measured here have CDs between 140 nm and 155 nm CDs.

To perform a more detailed analysis in this range, optical TFFM simulations were obtained at 2 nm CD increments from 146 nm to 156 nm and for illumination NAs varying between 0.35 to 0.39. Comparison of the difference between the experimental left intensity peaks with simulated left intensity peaks for a 10 nm range of CDs showed that the 0.36 illumination NA data matched closest to the experimental data. This test indicated that the effective illumination NA is in fact closest to the 0.36 value. The simulated TFFM profiles for 0.36 illumination NA are presented in Fig. 16 and show good qualitative agreement with the experimental TFFM profiles in Fig. 14.

Based on analysis of the simulated and the experimental TFFM profiles we evaluated the CD values for the targets selected. Figure 17 shows the normalized left peak focus metric value as a function of CD for both the simulations and the experiments. The curve in the figure labeled simulation is a plot of the simulated left peak focus metric values versus the CD values used as inputs to the simulations. The curve labeled experimental is a plot of the experimental left peak focus metric values versus the SEM measured CD values. By matching the intensity of the experimental focus metric value with the simulated focus metric value, CDs for all of the selected targets can be evaluated based exclusively on modeled results without reference to the SEM data as seen in Fig. 18. In this initial attempt to quantitatively measure CDs with the TFFM method based strictly on modeling results, good agreement was observed between the SEM and the optical TFFM method.

4. SUMMARY

Much emphasis is given to achieving uniform spatial intensity in optical instruments, which use a Köhler illumination scheme. Although the illumination may have uniform spatial intensity, it may not have symmetric angular illumination (Köhler factor 2 - KF2). For metrology applications, it is critical to obtain angular illumination homogeneity to improve measurement accuracy.

In this paper we presented a new method for evaluating the angular illumination homogeneity in an optical instrument using the through-focus focus metric (TFFM) method. The TFFM is defined as the focus metric value (sum of slopes) from an optical image as the target is stepped through the focus. For this analysis we divided the illumination into negative and positive angles of illumination. The final optical image is the incoherent sum of the images formed by all the negative and positive angles of illumination. For the target geometry and optical configuration used here, optical simulations showed that the highest contrast image was formed when the illumination was most asymmetric. Conversely, the lowest contrast image resulted when the images formed by the negative and the positive angles of illumination were most symmetric resulting in nearly zero value of the focus metric. Using the optical simulations, we demonstrated that the angular illumination asymmetry proportionately increased the contrast (and hence the focus metric value). Based on this observation, an experimental illumination analysis was performed. To do this on an optical tool, the through-focus focus metric was evaluated on a grid across the field view. Analysis of the focus metric value at the lowest contrast point (lowest contrast image) across the field of view provided an estimation of the angular illumination homogeneity. An independent experimental test showed good agreement with the illumination analysis using the TFFM. To obtain satisfactory analysis the selection of the experimental parameters need to be optimized.

Using the same TFFM technique, we presented a detailed study to evaluate critical dimensions using a bright field optical microscope. The TFFM method showed good experimental nanometer sensitivity to changes in CD. With the aid of the optical simulations and SEM/SXM, the CDs were evaluated. The CD values evaluated optically showed reasonably good agreement with the SEM measured values.

ACKNOWLEDGEMENTS

The authors would like to thank the Office of Microelectronics Programs of NIST for financial support and International SEMATECH for wafer fabrication support. The authors also would like to acknowledge Robert Larrabee, James Potzick, Thomas Germer, Michael Stocker, Heather Patrick, Bryan Barnes, Egon Marx, and Mark Davidson for assistance and useful discussions.

REFERENCES

1. R. Attota, R. M. Silver, M. Bishop, E. Marx, J. Jun, M. Stocker, M. Davidson, and R. Larrabee, "Evaluation of New In-chip and Arrayed Line Overlay Target Designs," Proc. SPIE, Microlithography Vol. **5375**, p. 395 (2004).
2. R. Attota, R. M. Silver, T. A. Germer, M. Bishop, R. Larrabee, M. T. Stocker, L. Howard, "Application of Through-focus Focus-metric Analysis in High Resolution Optical Metrology" Proc. SPIE, Microlithography Vol. **5752**, p. 1441-1449, 2005.

3. T.A. Germer, and E. Marx, "Simulations of optical microscope images of line gratings," Proc. SPIE, Microlithography Vol. **6152**, 2006.
4. R. M. Silver, R. Attota, M. Stocker, M. Bishop, J. Jun, E. Marx, M. Davidson, and R. Larrabee, "High resolution optical metrology" Proc. SPIE, Microlithography Vol. **5752**, p. 67-79, 2005.
5. Y. Ku, A. Liu, and N. Smith, "Through-focus technique for nano-scale grating pitch and linewidth analysis" Optics Express **13**, p. 6699-6708, 2005.
6. R. M. Silver, M.T. Stocker, R. Attota, M. Bishop, J-J. Jun, E. Marx, M.P. Davidson, and R.D. Larrabee, "Calibration strategies for overlay and registration metrology," Proc. SPIE, Microlithography Vol. **5038**, p. 103-120, (2003).
7. Y.J. Shon, B.M. Barnes, L. Howard, R.M. Silver, R. Attota, and M.T. Stocker, "Köhler illumination for high resolution optical metrology," Proc. SPIE, Microlithography Vol. **6152**, 2006.
8. M. Davidson, "Analytic waveguide solutions and the coherence probe microscope," Proceedings Microcircuit Engineering 90, Leuven, Belgium, September 1990.
9. R. M. Silver, B. M. Barnes, R. Attota, J. Jun, J. Filliben, J. Soto, M. Stocker, P. Lipscomb, E. Marx, H.J. Patrick, R. Dixson and R. Larrabee, "The limits of image-based optical overlay metrology," Proc. SPIE, Microlithography Vol. **6152**, 2006.